Roll-to-roll manufacturing of integrated immunodetection sensors

Journal:	*ACS Sensors*
Manuscript ID	se-2020-00404t.R2
Manuscript Type:	Article
Date Submitted by the Author:	28-May-2020
Complete List of Authors:	Liedert, Christina; VTT Technical Research Centre of Finland Ltd, Biosensors Rannaste, Lauri; VTT Technical Research Centre of Finland Ltd, Biosensors Kokkonen, Annukka; VTT Technical Research Centre of Finland Ltd, Biosensors Huttunen, Olli-Heikki; VTT Technical Research Centre of Finland Ltd, Liedert, Ralph; VTT Technical Research Centre of Finland Ltd, Biosensors Hiltunen, Jussi; VTT TECHNICAL RESEARCH CENTRE OF FINLAND Hakalahti, Leena; VTT Technical Research Centre of Finland Ltd, Biosensors

Roll-to-roll manufacturing of integrated immunodetection sensors

Christina Liedert*, Lauri Rannaste, Annukka Kokkonen, Olli-Heikki Huttunen, Ralph Liedert, Jussi Hiltunen, Leena Hakalahti

VTT Technical Research Centre of Finland Ltd, Kaitoväylä 1, 90570 Oulu, Finland

Supporting information

ABSTRACT: Lack of functional integration and high manufacturing costs have been identified as major challenges in commercialization of point-of-care devices. In this study, roll-to-roll (R2R) fabrication process was developed for large-scale manufacturing of disposable microfluidic devices. The integrated, user-friendly device included plasma separation membrane for simple blood filtration, immobilised antibodies for specific immunodetection, microfluidics for plasma transport and reagent mixing, and a blister for actuation and waste storage. These functionalities were designed to be compatible with R2R processing, which was demonstrated using pilot scale printing lines producing 60 devices in an hour. The produced sensors enabled rapid (10 min) and sensitive (2 µg/ml) fluorescence based immunodetection of C-reactive protein from 20 µl of whole blood.

KEYWORDS: Roll-to-roll manufacturing, point-of-care, cyclic olefin copolymer, immunoassay, microfluidics, blood filtration

Roll-to-roll (R2R) manufacturing includes variety of foil-based processes in which additive and subtractive techniques are implemented to build functional structures on a continuous substrate, called a web. [1] A wide range of intermediate and final products are to date already manufactured by R2R processes, such as print media, labels, textiles, tapes, films and filters. [1] These examples illustrate the benefits of R2R fabrication as a technology supporting production in large volumes at low cost. Research in the field has lately focused on development of integrated R2R products such as smart packaging, flexible electronics e.g. solar cells and lighting elements, as well as sensors for healthcare applications. [2-7]

Point-of-care (PoC) diagnostic tests are used at, or near the site of patient care. Ideal PoC devices should be affordable, sensitive, specific, user-friendly, rapid and robust, equipment-free and deliverable to end user.[8,9] PoC devices are deceivingly simple to operate but in fact contain variety of innovations that enable miniaturization of complex laboratory protocols onto a small chip. One key technology is microfluidics, which enables controlled handling of small (nl-µL) liquid volumes and a pipette-free sample preparation. [10, 11] Despite of the advantages enabled by microfluidics and extensive research effort invested in it, surprisingly few microfluidic devices have been commercialized to date.[12,13] Besides to the non-technical reasons (funding and regulatory issues), lack of functional integration and high manufacturing costs have been identified as major challenges in introducing PoC devices to the price sensitive consumer markets. [11-13]

There are several methods and materials available for commercial scale manufacturing of microfluidic devices. Glass, silicon, and quartz devices are fabricated using photolithographic or wet-etching procedures followed by bonding with adhesive or acid in high temperatures. [14] The unit price of these devices is high for several PoC applications where the test devices often need to be disposable. Therefore, microfabrication of polymers has gained popularity. Injection molding is the leading technology for the fabrication of polymer microfluidics in a larger scale. [15] Another cost-effective methods are R2R hot embossing [15-18], R2R thermal imprinting[7] and R2R UV nanoimprint lithography [19] which can achieve similar production throughput as injection molding. From the perspective of system integration, R2R manufacturing offers several advantages to sensor field e.g. in-line integration of functional components such as printed electronics, power and light sources, and printed biomolecules.

Immunoassays have been widely implemented in various test formats including optical, electrical and mechanical sensors. [20] ELISA (enzyme-linked immunosorbent assay) tests are a standard, although laborious and time consuming method used in several laboratories. In comparison, point-of-care market applying immunoassays is dominated by lateral flow test strips where the analysed sample is transported by capillary action in a fibrous cellulose based material. Lateral flow assays have been criticized for lack of repeatability that arise from the materials as well as from inconsistent manufacturing processes involving manual assembly.[21] R2R fabrication can be fully-automated which despite of high initial equipment investment cost produces sensors in a very competitive unit price. R2R methods are being adopted to LFA production as well e.g. R2R dispensing is commonly used. In this study, we have

developed a process flow combining several R2R techniques to fabricate fully-integrated, low-cost microfluidic immunosensors for detection of C-reactive protein from whole blood. CRP is a biomarker that indicates infection, inflammation and tissue damage. [22]

RESULTS AND DISCUSSION

Roll-to-roll manufacturing of polymer microfluidics. A multistep, R2R manufacturing process for high-volume fabrication of integrated immunoassay devices (Fig. 1) was developed and demonstrated using pilot scale roll-to-roll printing lines (supplementary video 1, R2R manufacturing). COC was chosen as the base substrate due to its optical clarity, suitable thermoplastic properties (T_g =78 °C), assay compatibility, and availability in large quantities in a roll format.[23, 24]

R2R hot embossing is a large area patterning technique that was used to replicate microfluidic channels. The critical parameters affecting channel profile and dimensions are a combination of roller temperature, pressure and web speed. [25-28] Our optimised parameters for the microfluidic design (Fig. 2A) were: embossing temperature close to the Topas COC glass transition temperature Tg (78 °C), 63 kN/m nip line pressure and 0.3 m/min roller speed. These values do not correspond to the values reported in literature. Other studies that simulate R2R embossing by feeding a web or polymer sheet through pressurised rollers have used temperatures much higher than the glass transition temperatures which has resulted in higher replication fidelity between the mold and the channel. [27-29] Our study however takes into consideration tension control which is an important factor in all R2R processes. Due to the tension, increasing the temperatures above Tg would stretch and break the web. By increasing the speed, higher temperatures could be used but the replication fidelity suffered as a consequence. The most challenging structure in the design was the meandering channel (Fig. 3A, microfluidic mixer) where polymer had limited space to flow away from the mold during embossing. The structure had tendency to buckle upwards which is why higher pressures than typical embossing pressures were used (500 N/ cm, [15]). Based on our experiments, the complexity of the microfluidics has a critical influence on the selection of embossing parameters i.e. temperature, pressure and speed which are conditional from each other. Furthermore, tension control is an important parameter in R2R processes that should be considered in future studies.

Encapsulation of microfluidics is often the yield limiting step in device fabrication and thus a critical step in high volume production. [15] In this study, R2R solvent lamination of channels was demonstrated. A blank COC web (lid layer) was coated with mesitylene using gravure coating in the flexo printing unit. An anilox roll containing evenly sized little cups spread a controlled layer of solvent onto the web. 8 cm^3/m^2 of solvent was calculated to be transferred on web. Mesitylene dissolved the interphase of COC, which became consequently sticky, forming an adhesive COC. The sticky lid layer was then bonded with the COC web carrying the microfluidic structures by running the two webs through a moderately heated nip. Lamination step was preceded by an antibody dispensing step (Fig. 1A) and a major concern was that the printed antibodies would not survive the contact with solvent. However, as discussed later, the bioanalytical results show that antibodies could bind target analyte after the bonding. Partial denaturation of antibodies may have however occurred, and it was not tested whether other antibodies are equally resistant as the anti-CRP antibodies. Sheet level lamination of COC microfluidics with solvents has been described and found to be a good option for devices that need to tolerate high burst pressure or heat cycling required in PCR amplification. [26, 28, 30] Industrial scale R2R solvent based lamination machinery is however commercially available and used to bond multilayer films. As an alternative to liquid lamination solvent deposition from vapour phase was reported but the process is slow and requires very precise control of conditions [30,31] which might be difficult to achieve in a R2R process. We are not aware of other studies reporting R2R solvent bonding of microfluidics, although a hexadecane soaked elastomeric roller as inkpad for controlled solvent spreading was suggested previously.[28]

As a final process step, commercial blood filtration membranes were assembled onto the web using a pick-and place hybrid assembly process. Hybrid assembly of components is commonly used in electronic industry. Hybrid assembly pilot line allowed very accurate positioning of membranes in relation to the microfluidic channel inlet with alignment accuracy of ± 20 µm. The blisters providing the fluid actuation mechanism for the microfluidics were attached manually, a step which could also be automated. Blister could be part of the packaging e.g. adhesive with printed graphics that define the appearance of the device.

There are several reports describing high volume microfabrication of microfluidics, but the following steps required to create functional devices are typically performed manually piece-by-piece. Yet, back-end processing can amount for 80% of the manufacturing costs. [15] The merit of this study is the demonstration of an entire roll-to-roll fabrication process in manufacturing of integrated microfluidic devices on a single, flexible substrate (Fig.1C). Hybrid assembly of blood filters was the rate limiting process step. It took about 1 minute to dispense glue and UV cure one membrane, allowing fabrication speed of 60 devices per hour.

Characterization of the microfluidic devices. The microfluidic devices were characterized after the replication step and after the lamination step. Profile and dimensions of the hot embossed microfluidic channels were measured with a surface profilometer. Channel depths of 45 µm were achieved for 400 µm wide channels which represents 50% of the mold height (Fig. 2B,C). Other studies report 85% [27, 28] or even 100% [29] replication fidelity with 100 µm channel width but as discussed previously these studies used temperatures much above polymer Tg without controlled web tension. The repeatability of the embossing depth was determined by taking profilometric measurements from beginning, middle and in the end of 35 meter long web. The variation was found to be 2.5 %, similar as reported previously [17]. The R2R hot embossing process was thus found to be very repeatable and stable over time.

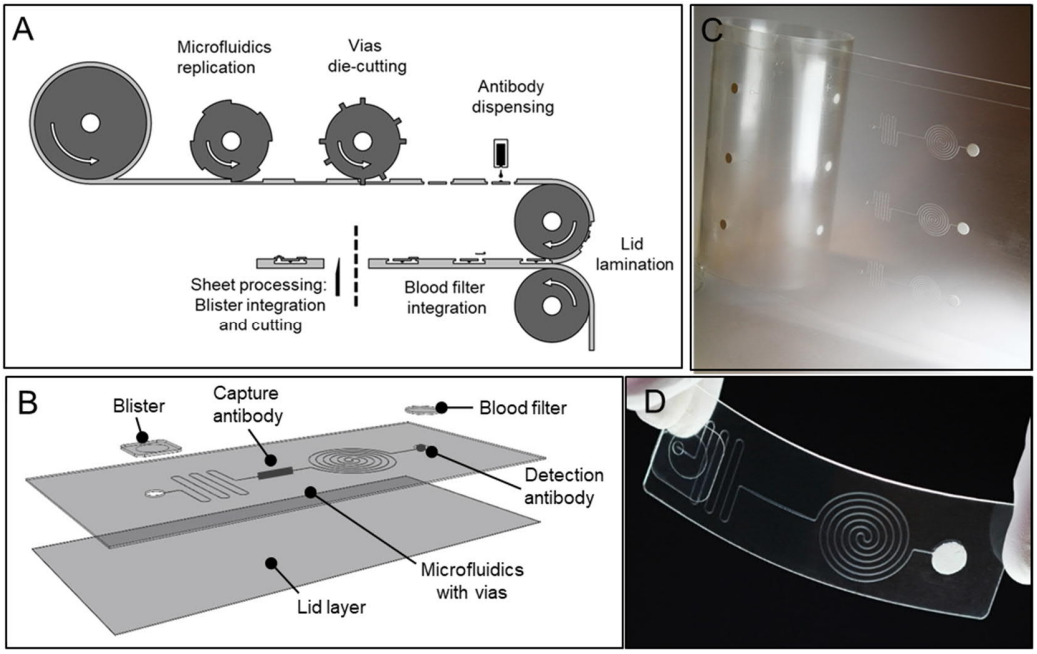

Figure 1. Roll-to-roll fabrication process for integrated microfluidic devices on COC. The consecutive R2R process steps (A) include hot embossing of microfluidics, die-cutting of vias, antibody dispensing to the microfluidic channel, lidding of the microfluidic layer with blank COC layer using solvent lamination, and finally hybrid assembly of blood filtration membranes above the inlet (supplementary video 1, R2R manufacturing). Blister integration and cutting were done manually but these steps can be automatized as well. The layer structure of the device is presented in (B) illustrating that microfluidic layer with cut through holes and integrated antibodies is phasing the blank lid layer, whereas filter and blister are assembled on the back side of the microfluidic layer. R2R processing resulted in functional microfluidic devices in a web format (C) which can be cut into flexible, disposable point-of-care devices (D).

Solvent lamination with another COC layer was used for lidding. The critical aspect in solvent lamination is the prevention of structural damage by melting of the microstructures. As seen in the microscope image Fig. 2E, the channel sides were sealed but the channels remained open. Further SEM investigation from a slit channel showed that the two COC layers had bonded together seamlessly (Fig. 2F). The sidewalls of the mold (Fig. 2B) as well as of the channels (Fig. 2C) were slightly slanted. This helps in the detachment of the mold from the polymer during embossing but negatively affects the bonding. The solvent dissolves the slanting in part but further calendaring i.e. running the web through a nip is required. Solvent bonding makes the channel edges rounded (Fig. 2F).

Self-contained microfluidic device. One of the challenges that all PoC devices face is how to make the devices user-friendly. Broad adaptation of microfluidic devices is limited by necessity of bulky, expensive off-chip instruments for liquid transport such as peristaltic, syringe and pneumatic pumps. On a low-cost, easy-to-use PoC device, the liquid flow is ideally achieved by capillary flow so that no external equipment is needed. This can be achieved for example with fine microfluidic structures that create high capillary pressure within the channel. [32] However, required limit values < 50 µm in width and > 100 µm in depth are difficult to fabricate with roll-to-roll embossing. Short embossing time and the thickness of the polymer web (375 µm) limit the R2R achievable channel depth whereas width of parallel structures is limited by the polymer flow around the mold during embossing, opposed to removal techniques such as etching.

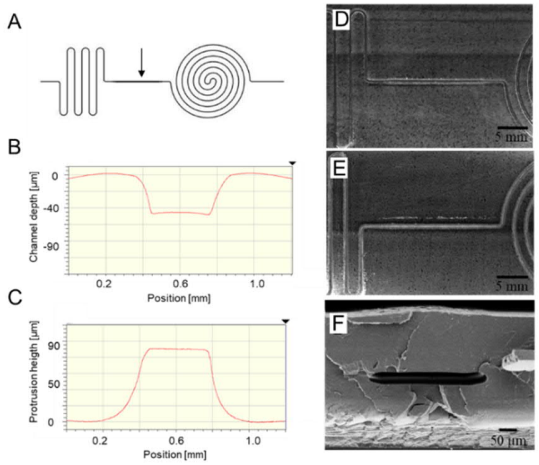

Figure 2. Microfluidics (A) was replicated using a steel tool which had a relief height of 90 µm (B). The embossed channel had height of 45 µm (C). Channels were imaged with microscope before (D) and after solvent (E) lidding. The cross-cut of the channel was further imaged with SEM showing tight seal between two COC layers (F).

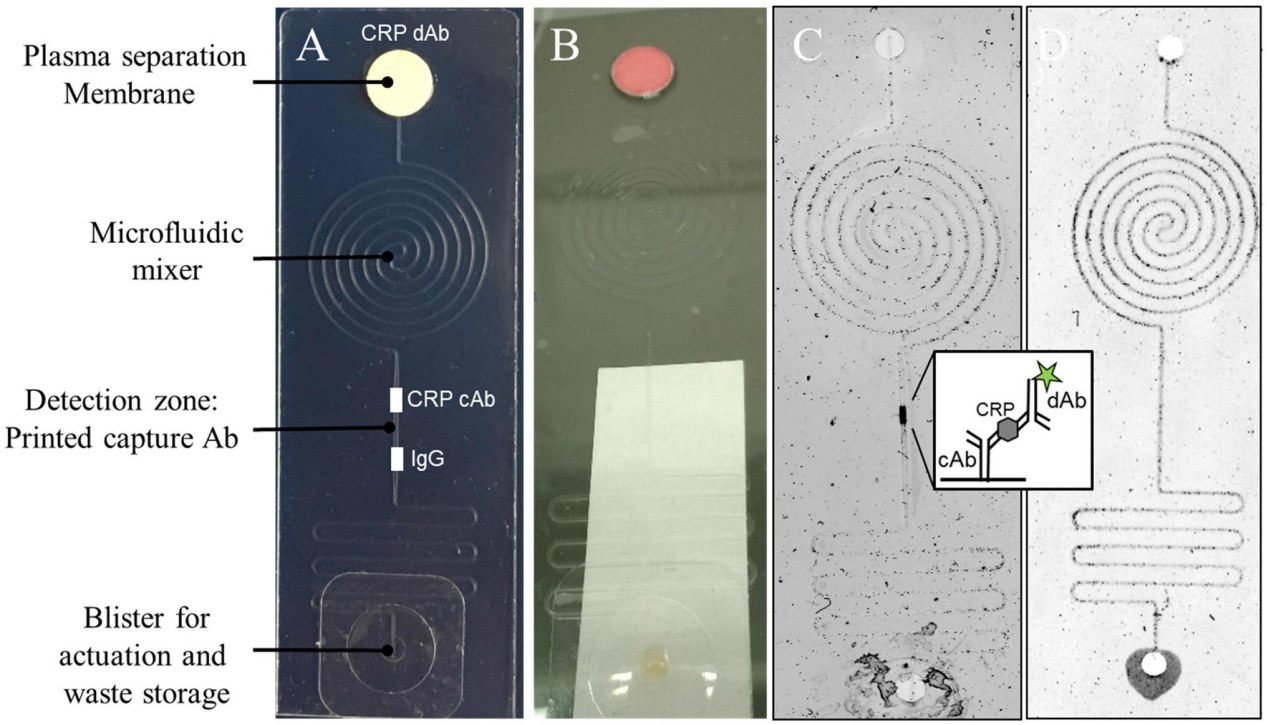

Figure 3. Fully-integrated microfluidic immunoassay chip included microfluidics for sample transport and mixing, blister for fluid actuation, printed anti-CRP capture antibodies (cAb) and mouse Immunoglobulin G (IgG) as negative control, and labelled detection antibody (CRP dAb) under the plasma separation membrane (A). 20 µl whole blood spiked with 2 µg/ml of CRP was added on the membrane. Blister assisted actuation enabled hemolysis free plasma separation through the filter and flow through the microfluidic channel (B). White paper was placed under the device for better colour visualisation. Plasma flow 10 minutes (± 1 min) through the channel after which the results of the two-site CRP immunoassay (illustration in 3C) was analysed with a fluorescence scanner. Fluorescence scan image shows successful CRP detection at the detection zone where CRP cAb was immobilised whereas no signal was generated at the negative control line where IgG was immobilised (C). The same blood sample was tested without added CRP antigen to ensure that the donor blood did not contain detectable amount of CRP (D). Filter and blister were removed prior to scanning.

If the structures are very close to each other channels become very shallow and the channel shape deforms. To circumvent these design restrictions and allow simple fluidic transport, a finger-actuated blister pump was attached to the outlet (Fig. 3A). Pushing the blister down and letting it return created negative pressure within the channel which pulled the sample through the channel until the sample and some additional air filled the blister chamber (see Supplementary video 2, device operation). Similar "finger-powered" pumping elements have been reported previously for droplet microfluidic applications. [33, 34] The reported pump fabrication methods however require complex and expensive lithographic and CNC milling. Here, we applied commercial touch screen membrane switches as blisters that were hot embossed on PET sealed with a pressure sensitive adhesive, and integrated to the microfluidic devices by simply pressing them against the devices. Furthermore, the blister dome serves as a convenient waste storage after actuation since the plasma does not come in contact with fingers or an instrument that could be used to push the blister down.

The blister assisted actuation was vital for blood filtration success of the presented microfluidic device. A commercial plasma separation membrane was assembled on top of microfluidic inlet to enable removal of blood cells (Fig. 3A, B). Blood cells are often a source of variability in bioanalytics [35] which is why increased costs due to a specialized filter material and additional manufacturing step is justified. An air gap formed between the microfluidic surface and the membrane (Fig. 1B) which prevented plasma flow to the channel by gravity alone. The strong pull generated by the blister allowed plasma to enter the channel and flow through it. It is important to note that the blister properties had to be optimized taken into account the properties of the blood filter, sample volume and microfluidic design to guarantee hemolysis free filtration (Fig. 3B). The diameter and the wall thickness of the blister determine force of the negative pressure generated in the channel. If too weak, the blister was not able to pull plasma completely into the device. If too strong, hemolysis occurred and biomolecular binding was not kinetically favorable resulting in weak signal. Furthermore, meandering channels were added to the microfluidic design to increase the flow resistance. We concluded that a blister diameter of 13 mm, height of 2.6 mm and thickness of 0.125 mm resulted in good assay performance as well as removed plasma and unbound label remains from the channel.

The device performance was demonstrated using CRP immunoassay as a model. A two-site, non-competitive immunoassay [36] using a fluorescence labelled secondary antibody was applied in the detection of CRP. The CRP capture antibody was passively immobilized using isopropanol containing ink on the detection area to enable binding of the antigen in a specific location. A detection antibody labelled with green fluorescence dye was reversibly immobilized at the inlet of the channel, under the blood filter, with a help of sucrose containing ink (Fig. 1B). Integration of reagents on-chip enabled add-just-a sample type of device operation. The assay was performed (Supplementary video 2, device operation) by first pushing the blister down for 30 seconds to remove the air from channel after which 20 µl of whole blood spiked with 2 µg/ml of CRP was sampled on top of the membrane. Plasma was allowed to filter along the asymmetric membrane for 1 min before the blister was released. Plasma entered the channel and solubilized the detection antibody after which the labelled antibody were mixing and binding CRP in a passive micromixer (Fig.3A). CRP bound to the detection antibody was captured on the detection zone by the capture antibody forming the two-site immunocomplex (illustration in Fig.3C). Excess label and plasma were pulled within blister chamber after which the fluorescence signal was measured (Fig. 3C). As Figures 3C, 3D show, the device would further benefit from surface passivation to prevent unspecific attachment of the label to the channel which should be addressed in future development. Duration of the analysis was approximately 10±1 min since manually operated blister caused some variability in the flow speed. Therefore, to increase the assay repeatability and potentially to perform quantitative analysis, integration of mechanical actuator to a reader instrument would be beneficial.

CONCLUSION

This study demonstrates that R2R processing is a viable option for high-volume fabrication of integrated microfluidic sensors. Automation increases the reproducibility and throughput of sensor fabrication. However, technology has limitations that may affect the choice of materials and microfluidic design freedom, compared to the lithographic methods which are commonly used at the prototyping phase. We anticipate that this technology enables development of novel diagnostic platforms which utilize the system integration potential of the R2R techniques. Disposable, low-cost microfluidic devices could be integrated with other printed functionalities such as printed electronics, optical structures, printed power sources, electrochromic displays and hybrid assembled MEMS components.

EXPERIMENTAL SECTION

R2R hot embossing of microfluidics. To prepare a replication mold, microfluidic designs were first drawn with a commercial CAD software (Rhino3D from McNeel, Spain). The mold included six copies of the microfluidic channel and symbols needed for accurate alignment in different process steps (Fig. 4). The large area steel mold (300 mm x 410 mm) was fabricated by wet etching with a feature height of 80 µm as described in [17]. The etched alignment marks were further ablated with Nd:YAG laser (JK-100-FL, GSI, UK) to increase surface roughness of these patterns resulting in higher optical contrast of the patterns on the embossed web. For laser processing a power of 2 W, wavelength of 1064 nm, speed of 3000 mm/min and recol/focus lens 76/76 mm were chosen. The steel shim was laser welded into a shape of a closed cylinder. Finally, the cylinder was installed to the hot embossing unit of the roll-to-roll pilot line (Coatema, Germany, Fig. 5).

Cyclic olefin copolymer COC (Tekniflex COC 240, prepared from TOPAS 8007-04, Tekni-Plex Europe N.V) was chosen as substrate material. The thickness of the commercial COC was 240 µm and width 300 mm. The web was guided along the embossing cylinder prior to the nip, resulting in a short (12 s) preheating step. The web path in the pilot line was 10 meters which was kept under constant tension during the embossing. The optimized hot embossing parameters were as follows: The temperature on the surface of the hot embossing cylinder was 78-82°C and on the surface of the counter pressure cylinder 75°C. The channel profile was found to be best with a nip line pressure of 63 kN/m and the web speed of 0.3 m/min.

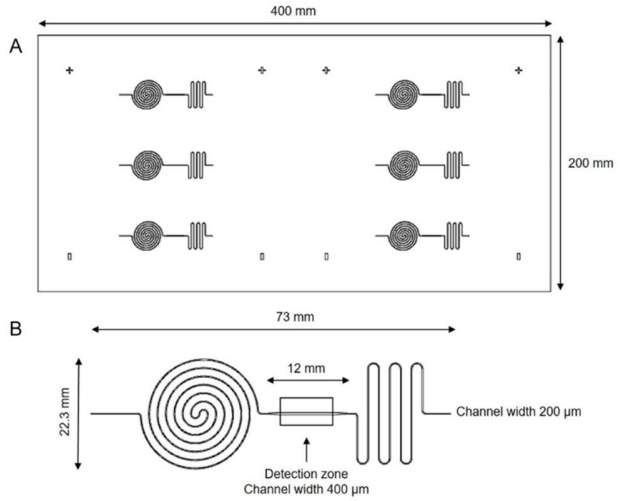

Figure 4. The embossing tool (A) consisted of 6 copies of the microfluidic device (B) as well as alignment marks for R2R dispenser (+ sign) and pick-and -place hybrid assembly line (□ sign).

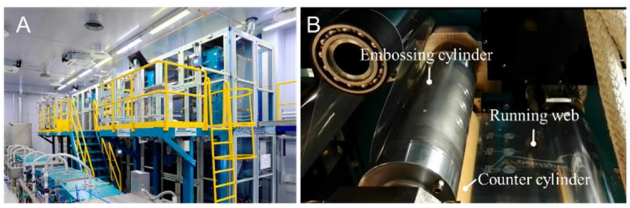

Figure 5. R2R replication of microfluidics was performed with a pilot printing line (A) using a hot embossing unit (B). A COC web was guided between oil heated embossing cylinder and counter pressure cylinder.

Rotary die cutting of vias. The backside of the hot embossed COC web was laminated with a liner (Nitto LensGuard SPV756TR_22 adhesive tape). The steel tool for die cutting

(Electro-Optic Gold line with 0.48 mm air gap) was prepared by wet etching and grinding with computer numerical controlled (CNC) milling. The rotary die cutting process was performed with Delta ModTech Rotary Converting System (Fig. 6) with a web speed of 1 m/min. More specifically, the cutting step was performed by kiss cutting [37], in such a way that the COC web was cut through, but the backing liner was left intact. By unpeeling the adhesive liner, the cut waste was simultaneously removed from the web. The vertical movement of the web was adjusted with automated web control, however horizontal alignment of vias with the microfluidic channels was performed manually. The measured alignment accuracy was 500 µm with a repeat length of 409.575 mm.

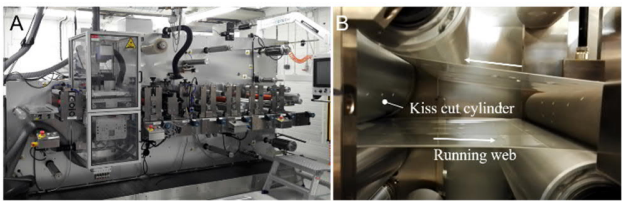

Figure 6. R2R cutting of vias was performed with a pilot scale converting line (A) using a die-cut unit in registry (B). Replicated COC web was bonded with an aligner foil prior cutting to allow controlled waste removal after cutting.

R2R Dispensing of antibodies. CRP capture antibody (hCRP monoclonal antibody, clone 6404, Medix Biochemica, Finland), and mouse IgG (Jackson Immunoresearch Europe Ltd) which was used as a negative control, were dispensed to the microfluidic channel with R2R dispenser (Delilah, Ginolis, Finland, Fig. 7). The instrument had only one dispensing head and pump so the two antibodies were dispensed in separate R2R runs. Antibodies were dispensed directly to the detection zone (Fig. 4B) as 3 x 2.5 nl droplets, with 300 µm drop spacing. Both CRP antibody and mouse IgG containing inks composed of 0.5 mg/mL of antibody, 1% isopropanol, 0.1% Tween20 in 12 mM PBS buffer pH 7.4.

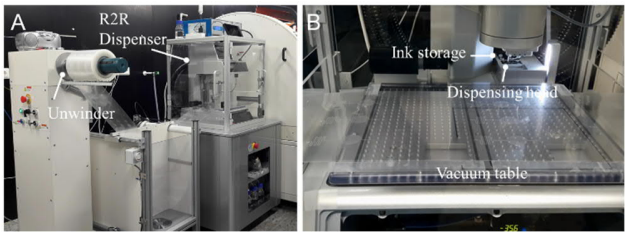

Figure 7. Roll-to-roll dispenser (A) was used to print antibody inks to the microfluidic channels (B). Web was held in place during dispensing by anchoring the web with a vacuum.

R2R Solvent lamination. R2R solvent lamination was performed using R2R flexo-printing technique, [38] (Fig. 8B). As anilox roll (Sächsische Walzengravur GmbH) the following measured engraving parameters were chosen: 41 lines/cm, stylus angle 110° and cell volume 24,7 cm^3/m^2. The anilox cylinder was used to transfer solvent (mesitylene, Sigma Aldrich) from an ink tray onto the cover layer web with the speed of 0.5 m/min. Solvent dissolved the upper most surface of the COC web transforming it to a sticky state. The channel layer was brought in contact with the solvent treated cover layer in a nip which was formed between flexo sleeve (full coverage rubber sleeve) and impression cylinder made of steel (Fig. 8B). After the first lamination step, the combined foils were guided through a second heated nip (upper cylinder 60°C and lower cylinder 42°C) in order to finalize the bonding. The web was then rewound to a core with inner diameter of 6 inches. A larger than typically used core was selected in order to reduce curvature and bending radius of the laminated web, and hence reduce environmental stress cracking of COC that residual mesitylene in the laminated film might induce.

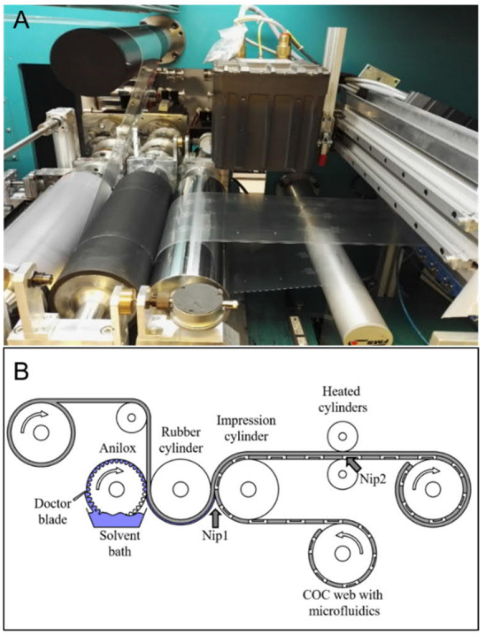

Figure 8. R2R solvent lamination (A) and illustration of the process (B).

R2R Hybrid assembly of blood filtration membranes. Datacon EVO 2200 (BE Semiconductor Industries, Netherlands) R2R pick-and-place system was used to stop-and-go assemble blood filtration membranes on the laminated COC web (Fig.9). Vivid plasma separation membranes GX (PALL Corporation, NY, USA) were cut with a biopsy puncher (Integra Miltex, France) into 8 mm diameter discs and placed onto a tray (Fig. 9B). A suction tool (Fig. 9C) picked the membranes and placed them on top of the inlet using the inlet hole for alignment positioning. Machine vision software used the square like alignment marks (illustrated in Fig.4A) for recognition of web position and wound the web to the correct position after each stop-and-go step. UV-curable glue (Loctite 3525, Henkel adhesives, USA) was dispensed using a syringe needle with pattern spindle speed 100%, 1 mm/s from a height of 0.125 mm above the web. After the glue was dispensed and the filter patch placed on top, UV curing was applied for 22 s. An actuation blister with diameter of 13 mm, 6.2 (±0.2) mm height and 125 µm thickness (hot embossed on PET attached to 3M adhesive tape, Screentec Ltd, Finland) was attached manually on top of the outlet hole. Two kinds of alignment marks were needed for accurate positioning. A rectangular symbol embossed on the web (Fig.4A) was used for winding

the web in correct position inside the hybrid assembly line. Secondly, for controlling the dispensing of the glue around the inlet hole the outlines of the inlet were used for alignment. After the filter assembly the web was rewinded to a roll. Blister assembly and cutting to individual devices were done in this study manually (Fig. 1A).

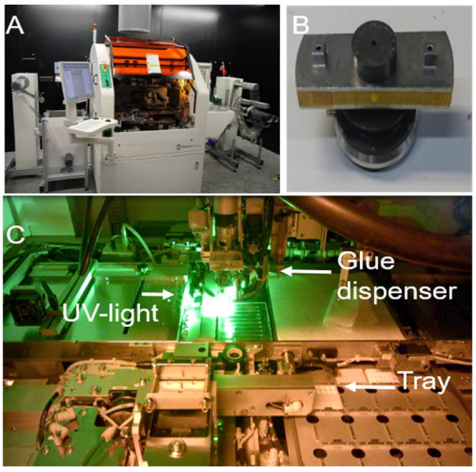

Figure 9. Hybrid assembly of blood filtration membranes was performed with Datacon pick-and-place line (A). Filters were picked up from a tray (B) with a vacuum tool (B) and placed in correct position after which UV-curable glue was dispensed around the membrane and cured with UV light (C).

CRP Immunoassay. Anti-CRP monoclonal antibody, clone 6405 (Medix Biochemica, Finland) was labelled with Alexa 546 fluorophore according to manufacturer's instruction (Molecular Probes, Thermo Fisher Scientific). 50 µg/ml (1 µl) of labelled antibody suspended in 15% sucrose, 0.1% Tween20 in 12 mM PBS with pH of 7.4 was pipetted to the inlet prior to the attachment of the blood filter membrane. 2 µg/ml of CRP antigen (BBI solutions, UK) was spiked to 20µl whole blood. Venous blood samples were obtained from healthy male and female donors from Finnish Red Cross blood service. The test set included a sample without added CRP to ensure that donated blood did not contain measurable amount of internal CRP. The microfluidic chip was operated as follows (supplementary video 2, device operation): The blister was pressed down either with a finger or with the blunt end of a pen. After 30 seconds, 20 µl of CRP spiked blood was added with a pipet or a disposable capillary tube (MICROSAFE, SAFE-TEC Clinical Products LLC, USA) on the blood filtration membrane. The blister was kept pressed down for an additional 1min to allow time for plasma separation through the membrane, after which the blister was allowed to return to the original shape. Negative pressure within the microfluidic channel pulled the filtered serum through the microfluidic channel until the chamber of the blister. The blister actuation pulled air after the sample had entered the chamber which assisted removal of plasma and label residues within microfluidic channel. The immunoassay device was scanned with a fluorescence scanner (Typhoon Trio, GE Healthcare) after the assay performance. Scan parameters were 450 PTM, 50 res. Blister and filter membrane were removed prior scanning.

Characterization. Profile measurements of the hot embossed microfluidic channels were performed with a stylus profilometer (Dektak, Veeco Instruments Inc, USA) with measurement length of 2000 µm and time of 15 s. After the lamination, the cross section of the channel was imaged with a scanning electron microscope (SEM) (Neoscope JCM-5000, JEOL, Japan), with voltage of 10 kV and zoom of 170. A channel sample cut for SEM imaging was prepared by dipping it into liquid nitrogen and bending it when the plastic laminate cracked smoothly. Before imaging, a thin gold layer was deposited on top of the sample by using a sputter coater (SC502 Sputter Coater, Quorum Technologies, Ltd, UK) with current of 10 mA and deposition time of 120s.

ASSOCIATED CONTENT

Supporting Information is available free of charge via the Internet at http://pubs.acs.org." Videos show R2R manufacturing of the integrated sensor and sensor operation.

AUTHOR INFORMATION

Corresponding Author

* E-mail: christina.liedert@vtt.fi

Author Contributions

CL, conceptualization, project administration, methodology, investigation, writing the original draft; LR, AK, OH, RL, methodology, investigation, visualization, review & editing; JH, LH methodology, Funding acquisition, review & editing.

Notes

The authors declare no competing financial interest.

ACKNOWLEDGMENT

The financial support from European Regional Development Fund for project "Developing production methods for rapid diagnostics and sample handling". Part of the facilities used were provided by the Academy of Finland Research Infrastructure "Printed Intelligence Infrastructure (PII-FIRI, grant no. 320020). The work is part of the Academy of Finland Flagship Programme, Photonics Research and Innovation (PREIN), decision 320168.We also wish to acknowledge VTT's pilot line operators and laboratory technicians and engineers, Jaakko Pennanen, Pentti Korhonen, Mikko Hietala, Pekka Ontero, Jenni Tomperi and Sari Pohjonen for their valuable assistance.

ABBREVIATIONS

R2R, Roll-to-roll; PoC, Point-of care; CRP, C-reactive protein, COC, cyclic olefin copolymer, SEM, Scanning electrode microscope

REFERENCES

(1) Cresko, J.; Shenoy, D.; Liddell, H.; Sabouni, R. Roll-to-roll processing, Chapter 6: Innovating Clean Energy Technologies in Advanced Manufacturing. Technology assessments. In Quadrennial Technology Review 2015. Publisher: U.S. Department of Energy, 181-225.

(2) Juntunen, E.; Ihme, S.; Huttunen, A.; Mäkinen, J-T. R2R process for integrating LEDs on flexible substrate, IEEE Conference Publications on 2017 IMAPS Nordic Conference on Microelectronics Packaging (NordPac), 12-16.

(3) Park, J.; Shin, K.; Lee, C. Roll-to-roll coating technology and its applications: A review. Int. J. Precis. Eng. Manuf. 2016, 17, 537-550.

(4) Keränen, K.; Korhonen, P.; Rekilä, J.; Tapaninen, O.; Happonen, T.; Makkonen, P.; Rönkä, K. Roll-to-roll printed and assembled large area LED lighting element. Int. J. Adv. Manuf. Tech. 2015, 81, 529-536.

(5) Leung, S.F.; Gu, L.; Zhang, Q.; Tsui, K.H.; Shieh, J.M.; Shen, C.H.; Hsiao, T.H.; Hsu, C.H.; Lu, L.; Li, D.; Lin, Q.; Fan, Z. Roll-to-roll fabrication of large scale and regular arrays of three dimensional nanospikes for high efficiency and flexible photovoltaics. Sci. Rep. 2014, 7, 4243, 1-8.

(6) Nyein, H.Y.; Bariya, M.; Kivimäki, L.; Uusitalo, S.; Liaw, T.S.; Jansson, E.; Ahn, C.H.; Hangasky, J.A.; Zhao, J.; Lin, Y.; Happonen, T.; Chao, M.; Liedert, C.; Zhao, Y.; Tai, L.C.; Hiltunen, J.; Javey, A. Regional and correlative sweat analysis using high-throughput microfluidic sensing patches toward decoding sweat. Sci. Adv. 2019, 5, eaaw9906, 1-12.

(7) Hiltunen, J.; Liedert, C.; Hiltunen, M.; Huttunen, O.H.; Hiitola-Keinänen, J.; Aikio, S.; Harjanne, M.; Kurkinen, M.; Hakalahti, L.; Lee, L.P. Roll-to-roll fabrication of integrated PDMS-paper microfluidics for nucleic acid amplification. Lab. Chip. 2018, 18, 1552-1559.

(8) Drain, P.K.; Hyle, E.P.; Noubary, F.; Freedberg, K.A.; Wilson, D.; Bishai, W.; Rodriguez, W.; Bassett, I.V. Diagnostic Point-of-Care Tests in Resource-Limited Settings. Lancet. Infect. Dis. 2014, 14, 239–249.

(9) Mabey, D.; Peeling, R.W.; Ustianowski, A.; Perkins, M.D. Diagnostics for the developing world. Nat. Rev. Microbiol. 2004, 2, 231-40.

(10) Cui, F.; Rhee, M.; Singh, A.; Tripathi, A. Microfluidic sample preparation for medical diagnostics. Annu Rev Biomed Eng 2015, 17, 267-286.

(11) Whitesides, G. The Origin and the future of microfluidics. Nature 2006, 442, 368-373.

(12) Chin, C.D.; Linder, V.; Kia, S.K. Commercialization of microfluidic point-of-care diagnostic devices. Lab. Chip. 2012, 12, 2118-2134.

(13) Convery, N.; Gadegaard, N. 30 years of microfluidics. Review. Micro Nano Eng. 2019, 2, 76-91.

(14) Jia, Z.-J.; Fang, Q.; Fang, Z.L. Bonding of glass microfluidic chips at room temperatures. Anal. Chem. 2004, 76, 5597-5602.

(15) Becker, H.; Gärtner, C. Polymer microfabrication technologies for microfluidic systems. Anal. Bioanal. Chem. 2008, 390, 89-111.

(16) Peng, L.; Deng Y.; Yi, P.; Lai, Z. Micro hot embossing of thermoplastic polymers: a review. J. Micromech. Microeng. 2014, 24, 013001, 1-23.

(17) Liedert, R.; Amundssen, L.; Hokkanen, A.; Mäki, M.; Aittakorpi A.; Pakanen M.; Scherer, J.R.; Mathies, R.A., Kurkinen, M., Uusitalo, S.; Hakalahti, L.; Nevanen. T.; Siitari, H.; Söderlund, H. Disposable roll-to-roll hot embossed electrophoresis chip for detection of antibiotic resistance gene mecA in bacteria. Lab. Chip. 2012, 12, 333-339.

(18) Wang, X.; Liedert, C.; Liedert, R.; Papautsky, I. A Disposable, Roll-to-Roll Hot-embossed Inertial Microfluidic Device for Size-based Sorting of Microbeads and Cells. Lab. Chip. 2016, 16, 1821 – 1830.

(19) Leitgeb, M.; Nees, D.; Ruttloff, S.; Palfinger, U.; Götz, J.; Liska, R.; Belegratis, M.R.; Stadlober, B. Multilenght Scale Patterning of Functional Layers by Roll-to-Roll Ultraviolet-Light-Assisted Nanoimprint Litography. ACS Nano. 2016, 10, 4926-4941.

(20) Yager, P.; Domingo, G.J.; Gerdes, J. Point-of-care Diagnostics for global health. Annu. Rev. Biomed. Eng. 2008, 10, 107-44.

(21) Tisone, T.C.; O'Farrell, B. Chapter 8: Manufacturing the next generation of highly sensitive and reproduciple lateral flow immunoassay. In ed. Wong, R.C.; Tse, H.Y. Lateral flow immunoassay. New York: Humana Press, 2009, 131-156.

(22) Pepys, M.B.; Hirschfield, G.M. C-reactive protein: a critical update. J. Clin. Invest. 2003, 111, 1805-1812.

(23) TOPAS datasheet: https://topas.com/sites/default/files/files/Packaging_E_2014-06.pdf, 1-34.

(24) Nunes, P.S.; Ohlsson, P.D.; Ordeig, O.; Kutter, J.P. Cyclic olefin polymers: emerging materials for lab-on-a-chip applications. Microfluid. Nanofluid. 2010, 9, 145-161.

(25) Yeo, L.P.; Ng, S.H.; Wang, Z.; Wang, Z.; De Rooij, N.F. Micro-fabrication of polymeric devices using hot roller embossing. Microelectron. Eng. 2009, 8, 933-936.

(26) Velten, T.; Bauerfeld, F.; Schuck, H.; Scherbaum, S.; Landesberger, C.; Bock, L. Roll-to-roll hot embossing of microstructures. Microsyst. Technol. 2011, 17, 619-627.

(27) Ng, S.; Wang, Z. Hot roller embossing for microfluidics: process and challenges, Microsyst. Technol. 2009, 15, 1149-56.

(28) Miserere, S.; Mottet, G.; Taniga, V.; Descroix, S.; Viovy, S-L.; Malaquin, L. Fabrication of thermoplastics chips through lamination based techniques. Lab. Chip. 2012, 12, 1849-56.

(29) Metwally, K.; Robert, L.; Queste, S.; Gauthier-Manuel, B.; Khan-Malek, C. Roll manufacturing of flexible microfluidic devices in thin PMMA and COC foil by embossing and lamination. Microsyst. Technol. 2012, 18, 199-207.

(30) Mair, D.A.; Rolandi, M.; Snauko, M.; Noroski, R.; Svec, F.; Fréchet, J.M.J. Room-temperature bonding for plastic high-pressure microfluidic chips. Anal. Chem. 2007, 79, 5097-5102.

(31) Wan, A.M.D.; Moore, T.A.; Young, E.W.K. Solvent Bonding for fabrication of PMMA and COP microfluidic devices. J. Vis. Exp. 2017, 119: 55175, 1-9.

(32) Gervais, L.; Delamarche, E. Towards one-step point-of-care immunodiagnostics using capillary-driven microfluidics and PDMS substrates. Lab. Chip. 2009, 7, 3330-7.

(33) Lee, S.; Kim, H.; Lee, W.; Kim, J. Finger-triggered portable PDMS suction cup for equipment-free microfluidic pumping. Micro Nano Syst. Lett. 2018, 6, 1-5.

(34) Iwai, K.; Shih, K.C.; Lin, X.; Brubaker, T.A.; Sochol, R.D.; Lin, L. Finger-powered microfluidic systems using multilayer soft lithography and injection molding process. Lab. Chip. 2014, 14, 3790-9.

(35) Mielczarek, W.S.; Obaje, E.A.; Bachmann T.T.; Kersaudy-Kerhoas, M. Microfluidic blood plasma separation for medical diagnostics: is it worth it? Lab. Chip. 2016, 16, 3441-3448.

(36) Cox, K.L.; Devanarayan, V.; Kriauciunas, A.; Manetta, J.; Montrose, C.; Sittampalam S. Immunoassay Methods. 2019, In ed. Sittampalam, G.S.; Grossman, A.; Brimacombe, K.; et al., Assay Guidance Manual, 1-39.

(37) Buck, B.L. Rotary die cutting systems and method for sheet material. United States Patent US5388490A, United States Patent and Trademark office, 14 February 1995, 1-7.

(38) Kipphan, H. Handbook of print media: technologies and production methods. Springer, 2001, 976–979.

For TOC only